

Rheinisch-Westfälische Technische Hochschule Aachen
Institut für Bildsamer Formgebung

Title bla blubb
blubb bla

Hauptseminar

Paul Hibbe, B. Sc. RWTH
Matthias Nick, B. Sc. RWTH

Durchgeführt in der Abteilung Werkstoffmodellierung
im WS 2013/14

Betreuer: Univ. Prof. Dr.-Ing. Gerhard Hirt
Dipl.-Ing. Thomas Henke
Stephan Hojda, M. Sc. RWTH

Contents

| | | |
|----------|--|-----------|
| 1 | Introduction | 3 |
| 2 | Foundations | 4 |
| 2.1 | Open-die forging | 4 |
| 2.2 | Finite element method | 4 |
| 3 | Model process | 5 |
| 3.1 | Material data | 5 |
| 3.2 | Forging plan (ForgeBase) | 7 |
| 4 | Previous work | 10 |
| 5 | Material modeling | 11 |
| 5.1 | Recovery and recrystallization | 11 |
| 5.2 | Semi empirical material models | 14 |
| 6 | Validation | 16 |
| 6.1 | DEFORM-3D | 16 |
| 6.2 | FORGE | 16 |
| 6.3 | PEP/LARSTRAN | 16 |
| 7 | Summary | 17 |
| 8 | Outlook | 18 |
| | List of Figures | 19 |
| | References | 20 |

1 Introduction

2 Foundations

2.1 Open-die forging

Open-die forging is the oldest forging process and can be used to create a variety of final forms. It is an incremental, highly flexible metal forming process. The process typically involves two dies of simple geometry moving towards one another and thus forming the work piece. Open-die forging processes can be separated into four categories: upsetting, stretch forging, punching and hollow forging. This work, however, will focus on a stretch forging process.[DB07]

The incremental and flexible nature of open-die forging makes it suitable primarily to the manufacturing of small lot sizes or for the forming of parts that cannot be produced by other processes due to power and force limitations of these processes. Its primary use is in the preparation of cast ingots for further machining. By open-die forging, cavities from the casting process can be rectified and the needed material properties can be reached.[DHK⁺11]

2.2 Finite element method

The finite element method is a method to model, beside others, continuum mechanics of solid work pieces. The work piece is separated into discrete parts, called elements, which are themselves geometrically defined by nodes. While these nodes hold coordinates as information, the elements hold temperatures, stresses etc. Using material properties such as flow curves, friction, thermal conductivity and emissivity, the system's reaction to thermal and mechanical external loads can be calculated.

Due to the non-linear nature of the resulting equation system, only very simple models can be calculated analytically while most must be approximated numerically. Besides matters of usability, the numerical approach is the most important difference between available software packages. These are spread across a wide spectrum from academic systems with large freedom for the user to easy-to-use specialized tools for certain uses.

Table 3.1: Chemical composition of 1.4301

| C[%] | Cr[%] | Ni[%] | Si[%] | Mn[%] | P[%] | S[%] | N[%] |
|----------|-------------|------------|----------|-----------|-----------|----------|----------|
| max 0,07 | 17,00-19,50 | 8,00-10,50 | max 1,00 | max. 2,00 | max 0,045 | max 0,03 | max 0,11 |

Table 3.2: Constant process parameters (reference temperature 20°C)

| | | |
|----------------------|----------|------------------------|
| Poison | 0,3 | - |
| Thermal expansion | 0,000012 | [1/K] |
| Emissivity | 0,7 | - |
| Heat transfer coeff. | 4,5 | [W/(m ² K)] |
| Friction coeff. | 0,4 | - |
| Dissipation | 0,9 | % |

3 Model process

This work deals with modeling of an open die forging process with multiple passes. The material used is a common stainless steel. The process parameters are orientated on a plan for forging a block with four passes given by the forging simulation software ForgeBase. Important process parameters, besides the flow curves, are for example the material data, the height reduction during every pass, the movement of the die, meaning the kinematics, the process temperature, etc. The detailed process conditions are discussed in the following chapters.

3.1 Material data

The material used is a 1.4301 (X5CrNiMo18-10) stainless steel. It is an austenitic steel which contains high quantities of the alloying elements chrome and nickel (Table 1). Therefore it is non-corrosive, acid- and heat-resistant. The field of application is widely spread and reaches from the automotive industry up to the chemical industry [(DE08].

The chemical composition (in weight-%) of the material is as follows [met14]:

For the input in a simulation model the thermal material data is crucial, containing are the temperature depending thermal conductivity, the spec. heat capacity and the Young's modul, see Figure 3.1, 3.2, 3.3.

It is necessary that the data describes the whole temperature range of the process. Further parameters are set constant and are pictured in ??

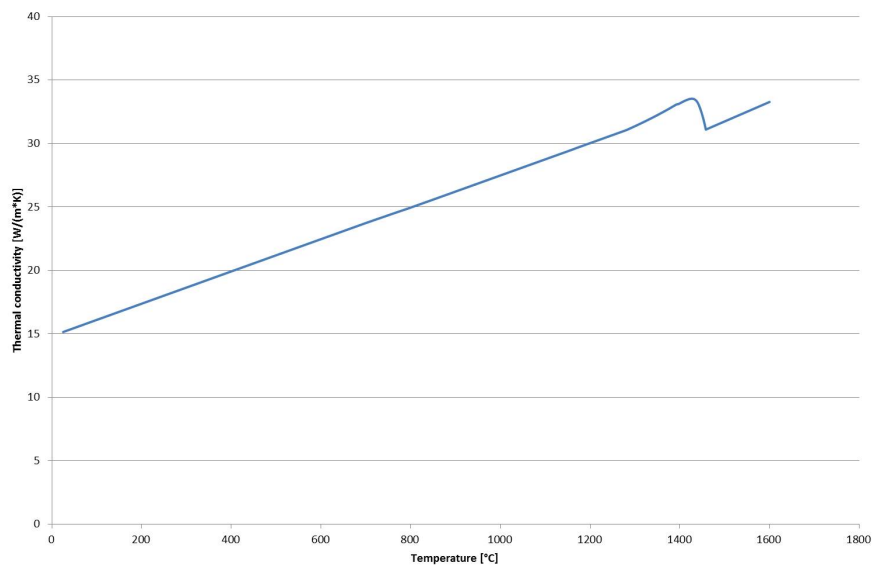


Figure 3.1: Thermal conductivity of 1.4301

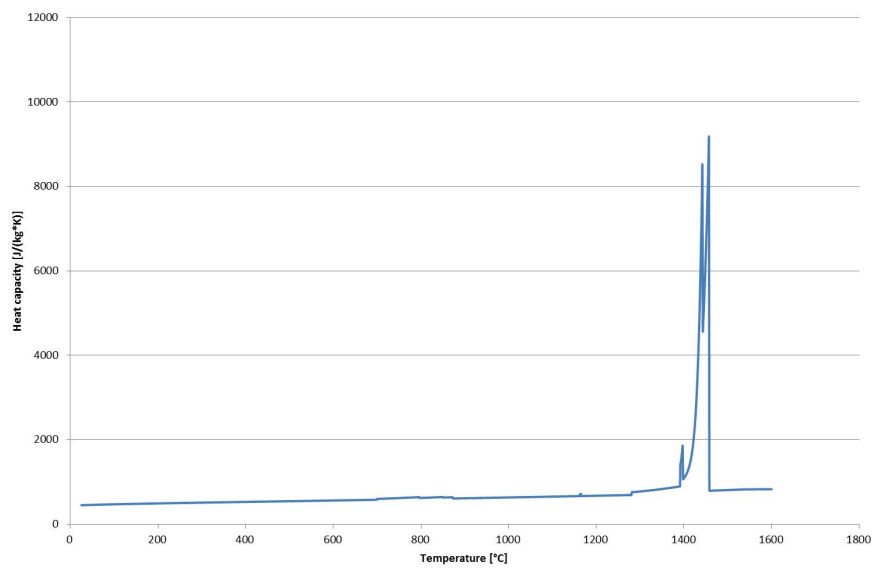


Figure 3.2: Heat capacity of 1.4301

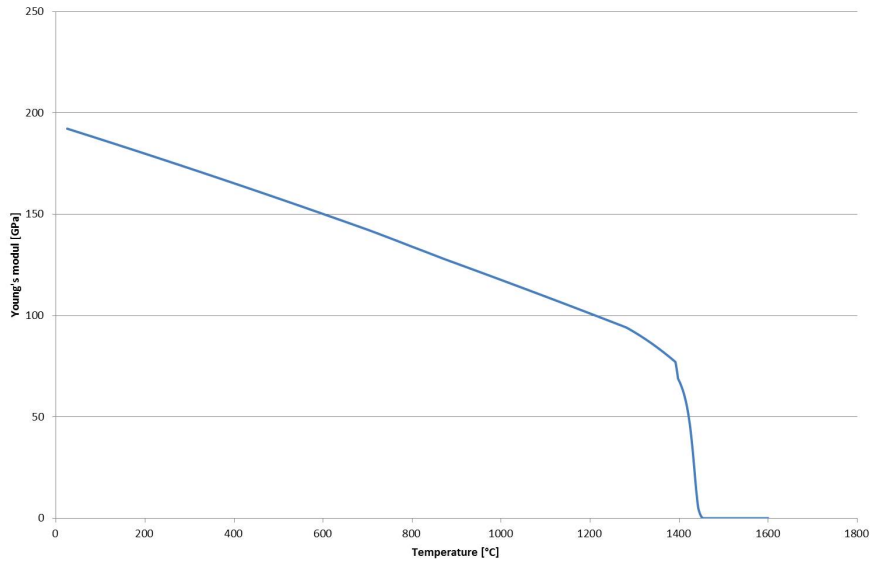


Figure 3.3: Young's modul of 1.4301

3.2 Forging plan (ForgeBase)

The settings of the forging simulation are based on the calculation of the forging software ForgeBase. The simulations are done for a four passes process on a block (workpiece - WP) with the dimensions of 150mm in height as well as in width and 600mm in length. However, only 400mm of the length are forged. The rest is provided for the manipulator to hold and move the WP. The WP is set as a plastic solid and is meshed with a brick mesh with 12544 elements. The upper and lower dies are set as rigid object. The manipulator is set up as a spring with a stiffness of 175 N/mm and the maximum clamping force of 222,4 kN. For detailed dimensions of the upper and lower die, as of the manipulator see refAppendix1.

The passes in the simulation vary in height reduction and bite ratio. Between the passes the WP is rotated in positive and negative direction with 90° rotation angle. The bottom die is fixed, though the top die moves with a speed of 80mm/s.

Moreover, the heat treatment before and during the process is of great importance. Before the first pass starts, the WP gets heated up to 1200°C for 2 hours. It is vital, that the WP does have a homogeneous distribution. During the forging passes, heat is getting lost by the effects of emission and the heat transfers to the dies. Because of that,

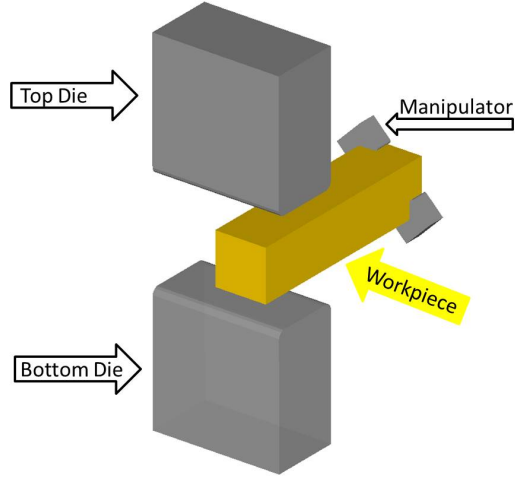


Figure 3.4: Illustration of the process setup from DEFORM

Table 3.3: Forging plan from ForgeBase

| Pass Nr. | Reduction [mm] | Height 1[mm] | Width 1[mm] | Height 2[mm] | Width 2[mm] | Rotation [°] |
|----------|----------------|--------------|-------------|--------------|-------------|--------------|
| 0 | 0 | 150 | 150 | 150 | 150 | 0 |
| 1 | 28 | 122 | 162 | 122 | 162 | 0 |
| 2 | 30 | 132 | 132 | 132 | 132 | 90 |
| 3 | 25 | 107 | 143 | 107 | 143 | -90 |
| 4 | 27 | 116 | 116 | 116 | 116 | 90 |

a second heat is necessary between the second and the third pass. The WP is heated up again to 1200°C within 1 hour. After the last pass the WP cools down upon air to room temperature.

4 Previous work

The described process has previously been investigated using Simufact.forming from simufact engineering gmbh. *Zusammenfassung Ergebnisse Yuwei*

5 Material modeling

This chapter deals with the concept of material modeling based on semi-empirical equations. At first there will be a short overview of the mechanisms of recovery and recrystallization and after that a review of common models describing the evolution of microstructure during hot forming and a way to integrate them into common FEM-software.

5.1 Recovery and recrystallization

The flow stress is highly dependent on microstructural softening and hardening mechanism during forming. In addition, these mechanisms are influenced by the temperature, strain rate and strain.

During hot forming, defects are generated within the crystal lattice. According to Gottstein [Got07] the defects can be distinguished respecting their dimensions. Especially one dimensional defects called dislocations, are the carriers of plastic deformation and therefore crucial for hot working. During hot deformation the density of dislocations rises and hence the resistance of the material to deformation rises too. At a certain point the stored energy in the material is high enough to induce dynamic recovery (DRV) or dynamic recrystallization (DRX). These mechanisms cause softening of the material.

DRV leads to equilibrium between hardening and softening. However DRX leads to a softened material. The effects of DRV and DRX can be well seen in the warm flow curve behavior, see 5.1.

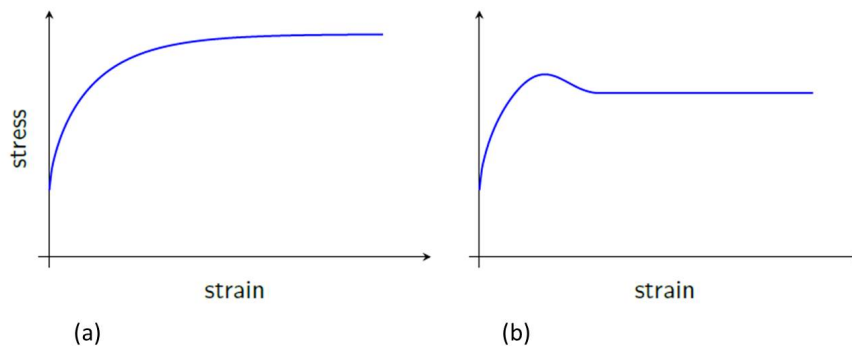


Figure 5.1: Warm flow curves when recovery (a) or recrystallization (b) is predominant [Loh10]

The softening effect of DRV and therefore the reduced level of stress with increasing strain is based on the rearrangement and annihilation of dislocations [Gottstein]. During DRX new grains are built and grow at spots with low specific energy. Both effects lead to a totally refined microstructure.

After hot forming, remaining dislocations can still store a great amount of energy. This energy can be enough to cause static recovery (SRV) or static recrystallization (SRX). These processes take place during heat treatment after warm forming. The softening effects are the same as in DRV or DRX. The driving force drops during SRV and SRX and only when there is enough energy stored, SRV and SRX lead to a fully refined microstructure.

After or parallel to SRV and SRX, grain growth (GG) can take place. The driving force is the reduction of stored energy. During grain growth the nucleated grains grow by using up the old grain structure.

5.2 gives a short summary about the recovery, recrystallization and grain growth mechanisms during warm forming.

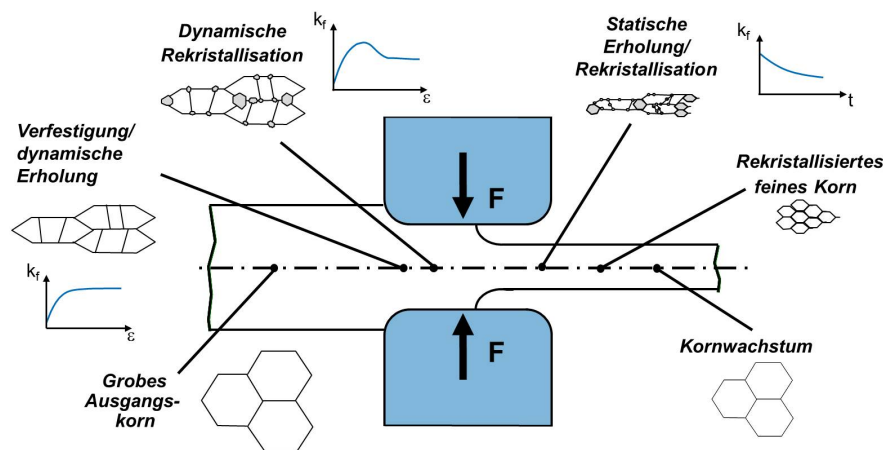


Figure 5.2: Recovery and recrystallization mechanisms during warm forming

The flow curves 5.3 are essential for the determination of the recrystallization kinetics and the fraction of recrystallized material. Therefore it is the basis for the creation of a microstructure model. At the IBF, flow curves are determined by isothermal compression tests at cylindrical specimens with an eight to diameter ratio of 1,5. For the 1.4301 tests have been carried out at temperatures ranging from 900 - 1250 °C and strain rates of 0,05 - 100 s⁻¹ 5.3.

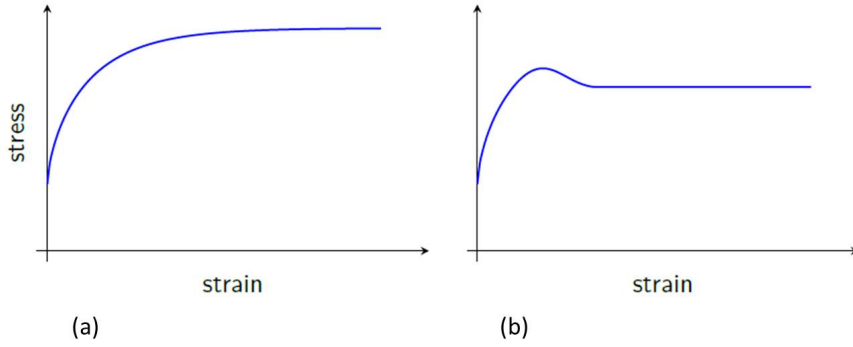


Figure 5.3: Determined flow curves of 1.4301 (temperature range: 900-1250°C)

For the semi empirical material model given by Deghan Manshadi [ARP08] the special strain values are of great importance. These strain states are seen in 5.4. There is the peak strain ε_p , the strain of steady state ε_{ss} , and not seen in 5.4 the critical strain ε_c which is located at 60% of the peak strain. The stresses at these characteristic points are also of importance.

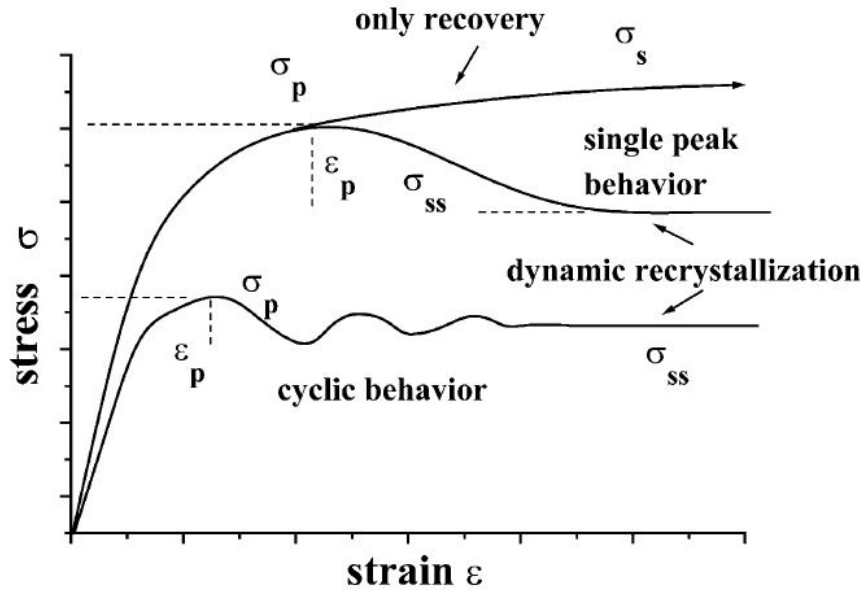


Figure 5.4: Warm flow curves with characteristic stress and strain points [MJJ03]

They can also be calculated by:

$$\varepsilon_p = 3,6 \cdot 10^{-3} d_{00} \cdot Z^{0,15} \quad (5.1)$$

$$\varepsilon_c = 0,6 \cdot \varepsilon_p \quad (5.2)$$

$$\varepsilon_{ss} = 0,00598 \cdot d_{00} \cdot Z^{0,1536} \quad (5.3)$$

5.2 Semi empirical material models

For the prediction of microstructural evolution semi-empirical models are used for many years. Lohmar and Karhausen gave a detailed overlook over the common models used in warm forming [Loh10][F.94].

The JMAK-equation is a way to calculate the fraction of recrystallization X 5.5 for the different recrystallization mechanisms DRX and SRX. In this work the equation for the calculation of DRX and SRX published by Dehgan Manshadi is used [ARP08].

$$X = 1 - \exp \left(\log(1 - 0,95) \cdot \left(\frac{\varepsilon_{eff} - \varepsilon_c}{\varepsilon_x} \right)^{1,3} \right) \quad (5.4)$$

$$X = 1 - \exp \left(\log(1 - 0,5) \cdot \left(\frac{t_{SRX}}{t_{50}} \right)^{1,1} \right) \quad (5.5)$$

Where t_{50} is the time where 50% softening took place:

$$t_{50} = 8 \cdot 10^{-9} \varepsilon^{-1,5} \cdot Z^{-0,42} \exp \left(\frac{375000}{R \cdot T} \right) \quad (5.6)$$

A lot of these models relate the stress behavior to the strain rate $\dot{\varepsilon}$ and the Temperature. A popular way to describe this is given by the Zener-Hollomon parameter Z [CH44]:

$$Z = \varepsilon \cdot \exp \left(\frac{Q}{R \cdot T} \right) \quad (5.7)$$

These equations lead to the determination of the grain size d_{DRX} and d_{SRX} [ARP08]:

$$d_{DRX} = 5916 \cdot Z^{-0,1748} \quad (5.8)$$

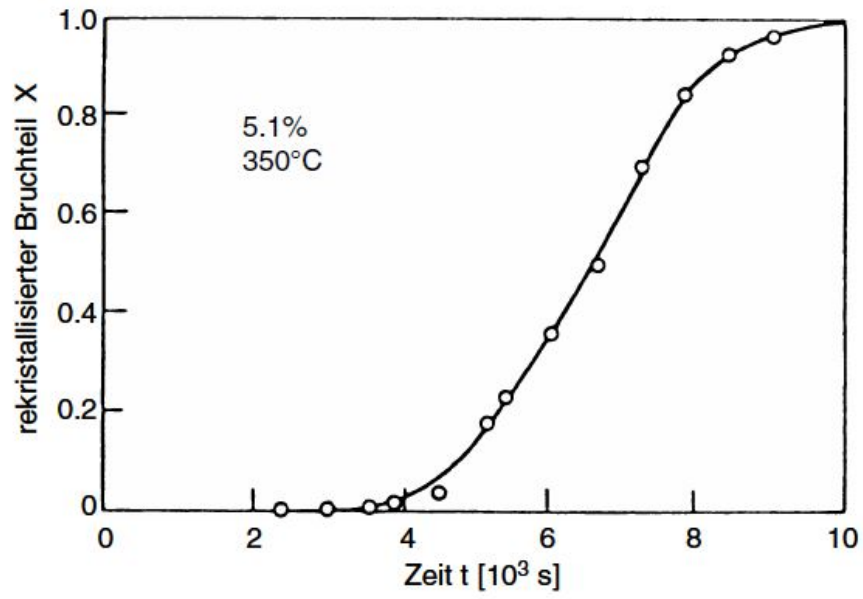


Figure 5.5: Fraction of recrystallization X [Got07]

$$d_{SRX} = 4,7 \cdot 10^2 \cdot \varphi_{SRX}^{-1} \cdot 100^{0,3} \cdot Z^{-0,1} \quad (5.9)$$

6 Validation

For the modelling of the described process, different software packages are available. Specifically, DEFORM-3D from Scientific Forming Technologies Corporation, Columbus, USA, FORGE from Transvalor, Mougins, France, and a combination of PEP (Pre- and Postprocessing Environment for Programmers) developed at IBF and LARSTRAN from LASSO Ingenieurgesellschaft mbH, Leinfelden, Germany have been used. These packages differ in their ease of use and freedom in modelling. A comparison of both usability and results will be made here.

6.1 DEFORM-3D

6.2 FORGE

6.3 PEP/LARSTRAN

7 Summary

8 Outlook

List of Figures

| | | |
|-----|---|----|
| 3.1 | Thermal conductivity of 1.4301 | 6 |
| 3.2 | Heat capacity of 1.4301 | 6 |
| 3.3 | Young's modul of 1.4301 | 7 |
| 3.4 | Illustration of the process setup from DEFORM | 8 |
| 5.1 | Warm flow curves when recovery (a) or recrystallization (b) is predomi- nant [Loh10] | 11 |
| 5.2 | Recovery and recrystallization mechanisms during warm forming | 12 |
| 5.3 | Determined flow curves of 1.4301 (temperature range: 900-1250°C) | 13 |
| 5.4 | Warm flow curves with characteristic stress and strain points [MJJ03] | 13 |
| 5.5 | Fraction of recrysralization X [Got07] | 15 |

References

- [ARP08] A., Deghan-Manshadi ; R., Barnett M. ; P.D., Hodgson: Hot Deformation and Recrystallization of Austenitic Stainless Steel: Part 1. Dynamic Recrystallization. In: *The Minerals, Metals & Materials Society and ASM International* (2008)
- [CH44] C., Zener ; H., Hollomon J.: Effect of Strain Rate Upon Plastic Flow of Steel. In: *Journal of Applied Physics Vol.15* (1944)
- [DB07] DOEGE, Eckart ; BERENS, Bernd-Arno: *Handbuch Umformtechnik*. 1. Berlin; Heidelberg; New York : Springer, 2007. – ISBN 978-3-540-23441-8
- [(DE08] (DEW), Deutsche E.: *1.4301 X5CrNi18-10*. http://www.dew-stahl.com/fileadmin/files/dew-stahl.com/documents/Publikationen/Werkstoffdatenblaetter/RSH/1.4301_de.pdf, 2008. – [Online; abgerufen am 31.01.2014]
- [DHK⁺11] DAHME, Michael ; HIRSCHVOGEL, Manfred ; KETTNER, Peter ; LANDGREBE, Dirk ; PISCHEL, Walter ; RAEDT, Hans-Willi ; RUILE, Christoph ; SCHLEICH, Michael ; WONDRAK, Jürgen: *Massivumgeformte Komponenten - Forged Components*. Landsberg am Lech : Hirschvogel Automotive Group, 2011
- [F.94] F., Karhausen K.: *Integrierte Prozeß- und Gefügesimulation bei der Warmumformung*, RWTH Aachen, Diss., 1994
- [Got07] GOTTSTEIN, Prof. Dr. G.: *Physikalische Grundlagen der Materialkunde*. 3. Aachen : Springer, 2007. – ISBN 978-3-540-71104-9
- [Loh10] LOHMAR, Johannes: *Modular Framework for the simulation of metal-physical events during hot working*, RWTH Aachen, Masterarbeit, 2010
- [met14] METALLOGRAF.DE, Werkstoffkartei: *1.4301 X5CrNi18-10*. <http://metallograf.de/>, 2014. – [Online; abgerufen am 31.01.2014]
- [MJJ03] M., El W. ; J.M., Cabrera ; J.M., Prado: Hot working of two AISI 304 steels: a comparative study. In: *Materials Science and Engineering* (2003)